Experimental investigation on the fundamental physical-layer capabilities for converged metro–access architectures using coherent transceivers

Experimental Investigation on the Ultimate Physical-layer Capabilities for Converged Metro-Access Architectures using Coherent Transceivers

GIUSEPPE RIZZELLI[1], MARIACRISTINA CASASCO[2], EMILIO RICCARDI[3], ANNACHIARA PAGANO[3], VALTER FERRERO[2], AND ROBERTO GAUDINO[2]

[1] *Photonext Center, Politecnico di Torino, Torino, Italy.*
[2] *Dipartimento di Elettronica e Telecomunicazioni (DET), Politecnico di Torino, Torino, Italy.*
[3] *Fibercop S.p.A.,Via G.Reiss Romoli, Torino, Italy.*

Compiled January 31, 2025

We present a fully-experimental investigation on the ultimate physical layer capabilities of future converged metro+access architectures using commercial coherent transceivers and ROADMs, which are placed at the boundary between the two network segments to implement all-optical routing of upstream and downstream wavelengths. For the access part, we focus on Passive Optical Network architectures, since they are the most commonly deployed and also the most demanding at the physical layer due to their very high loss and single fiber operation. In our experimental demonstration, we target very high bit rates (200G and 400G net data rate) and on the key physical layer scalability, such as maximum achievable optical distribution network loss as a function of available OSNR in the metro segments, reconfigurable optical add-drop multiplexer (ROADM) internal insertion loss and other possible impairments, like tight optical filtering or power level unbalances.

http://dx.doi.org/10.1364/ao.XX.XXXXXX

1. INTRODUCTION

In recent years, telecom network research has increasingly focused on developing innovative converged solutions to streamline network design, deployment, and management, particularly in the context of fixed-wireless convergence. Recently, some groups have also proposed all-optical convergence between the metropolitan and the access segments, focusing in particular on Passive Optical Networks (PON), i.e. considering an Optical Distribution network (ODN) based on single fiber tree (SF-T), enabled by the use of advanced modulation formats and coherent transceiver modules that allows much higher capacity and reach compared to previous direct-detection (DD) transceivers [1–3]. This research trend is justified by the following considerations:

- coherent PON (C-PON) is currently under active research analysis inside ITU-T working groups [4], industrial consortia [5] and academic labs [6, 7], focusing mostly on a PON bit rate upgrade towards 200+ Gbps rates
- thanks to the recent widespread deployment of Fiber-to-the-Home (FTTH) using PON, optical fiber terminations have become increasingly common in urban areas. PON is anticipated to almost entirely replace traditional copper access in the coming years, making this 'last mile' network of fibers as prevalent and ubiquitous as copper access has been over the past 80 years
- in the next decade, it can thus be interesting to use these SF-T-ODN terminations not only for "classical" FTTH, but also for some "super-users" requiring ultra high capacity (100+ Gbps), such as advanced 5G or future 6G fronthauling requirements, or SF-T-ODN usage for new applications, such as those largely discussed in [8] and in the next section of our paper.

Following all these considerations, we believe that the motivations for the introduction of coherent technologies in PON should not be limited to a pure bit rate upgrade, but also to a full re-thinking on how fiber access networks are organized and integrated with metropolitan networks.

In our previous works [2, 9–12], we already presented results on the topic of metro+access convergence using ROADMS. In particular, in [2] we show a detailed theoretical/simulative study on the physical layer scalability of these architectures, while our best experimental results so far were presented in [11, 12]. The current paper largely extends and elaborates on these Conference papers, presenting a much larger set of experimental results that covers several additional physical layers impairments compared to those addressed in [12]. Moreover, in this new paper we present a detailed brainstorming on the application scenario as seen from a telco operator perspective, with a future vision also on the implications for the networking layers and for the integration with x-hauling.

In the experiments reported in this work, we focus on demonstrating the ultimate physical layer capabilities, in particular in terms of maximum achievable ODN loss as a function of available optical signal-to-noise ratio (OSNR) in the metro segments and ROADM internal insertion loss and other possible impairments, such as tight optical filtering or ODN-induced power level unbalances. To this end, we experimentally consider only continuous point-to-point (PtP) bidirectional (BiDi) metro+access connections to and from the terminal of the access SF-T-ODN. However, regarding multiplexing solutions, several recent papers by other groups are currently addressing solutions suitable for C-PON, along two main possible research trends:

- time-division multiple access (TDMA) using burst mode coherent transmission and detection [13], where preliminary solutions show negligible performance penalty in terms of sensitivity between continuous mode and burst mode implementation.
- another alternative that has been proposed to achieve multiplexing in C-PON is also digital subcarrier multiplexing (DSCM) [1, 14], or even a mix of both (DSCM and TDMA)

As we will experimentally show in the rest of the paper, the achievable performance under continuous point-to-point bidirectional transmission in metro+PON are extremely promising and this, as previously said, is the key focus of our paper. The introduction of multiplexing (either TDMA and/or DSCM) will surely require further research works in the future, particularly for issues related to Erbium Doped Fiber Amplifier (EDFA) gain transients under burst-mode traffic and optoelectronic front-end linearity requirements under large optical power variations. Interestingly, this issue was already largely investigated in the past under several EU and Japan research projects and in slightly differently scenarios [15], [16].

All experimental results presented in the paper use deployed fibers in the Turin urban area, and commercial transceivers and ROADMs.

The paper is organized as follows. We start in Sect. 2 presenting an analysis on the possible network level implications that would derive from an all-optical merging between the metro and access segments. Then in Sect. 3 we describe the general scenario and the details of our experimental testbed. Finally, in Sect. 4 we show a large set of experimental results, addressing the physical layer scalability obtained in our experiments, considering different physical impairments in each Subsection.

2. NETWORK LEVEL CONSIDERATIONS

In optical access, the main deployed fiber infrastructures are either Point-to-Point (PtP) architectures or tree architectures with passive splitters (using SF-T-ODN and usually indicated as PON), with central offices as hub nodes and distributed edge locations in street cabinets (FFTCab) or directly in the final user premises (such as in FTTH). The metro segment is mainly a horseshoe logical infrastructure [17], with ROADMS in intermediate nodes where metro and access traffic is terminated and groomed. The need to reduce the number of central offices at the border between access and metro segments is driven by the need to lower operational costs, improve efficiency and reduce power consumption and is supported by the continuous upgrade of the coherent systems' performance, which allows much longer reach, flexibility and bit rates compared to DD legacy systems. However, this consolidation must be balanced with the need to support with appropriate infrastructure high-profile business customers who require high bandwidth and are located in peripheral locations (industry 2.0, edge data centers, point of presence of other networks). These customers often demand reliable and high-speed connections to convey their traffic into the core segment of the network. To cope with their future requirements together with the need of the wide FTTH platform for low traffic and low cost for residential customers, any new technology implemented should be compatible and coexist with legacy systems. This ensures that investments in existing fiber infrastructure are maximized and enables a seamless transition to new services without disruptions. This is important in the metro segments, where a huge capacity may have already been deployed before, and where customers seek to leverage their current assets without interruptions while gradually upgrading to more advanced solutions.

Another application that may require extremely high bit rate in fixed optical access is also x-hauling, in particular for the expected requirements of 6G [18] solutions that will likely involve massive use of MIMO and/or millimiter waves when implemented.

For a future merge of the two network segments, ROADM nodes in the metro section offer many degrees of flexibility using the spectral domain. This flexibility allows service providers to adapt the spectral load in order to accommodate the new traffic crossing transparently from the access segment, while maintaining the quality of service and the resilience needed for the transport application. New issues have obviously to be studied and solved: for instance, the inhomogeneity in the design rules of the two network segments' in this convergent metro-access scenario can induce inequalities in optical transmitted and received power levels (the last one is a concept not peculiar of metro segment), and in the signal to noise penalty (again, this concept is not known in access passive optical networks). The need for a common design imposes to take into account both received optical power (ROP) sensitivity limitations and amplified spontaneous emission (ASE) noise level (i.e. available OSNR), separately in upstream and downstream directions. Moreover the wavelength allocation of the carriers should address the dual approach of a metro network on a two-fiber infrastructure and a single-fiber access. Wavelength band separation is crucial to efficiently share the common infrastructure. In case of a flexible grid option, a spectral limited band allocation for channels originated and terminated in the remote access network terminations could be an interesting way to increase the available capacity, also considering that small penalties related to ROADM suboptimal filtering can be tolerated, especially when the ODN loss is not too high.

As previously mentioned, for the access segment the rest of the paper focuses on high ODN loss solutions, i.e. on the PON ITU-T ODN loss requirements above 29 dB. There are many other important access solutions that are not splitter-based, such as the BiDi family of solutions that is today widely used for 5G fronthauling. In this case, the physical layer constraints for a potential merging between metro and a future "coherent BiDi" solution would be less demanding, since the BiDi solutions ODN loss is significantly lower than for the PON situations. Even though not explicitly treated in our paper, most of the result shown in the rest of the paper would be applicable also for a

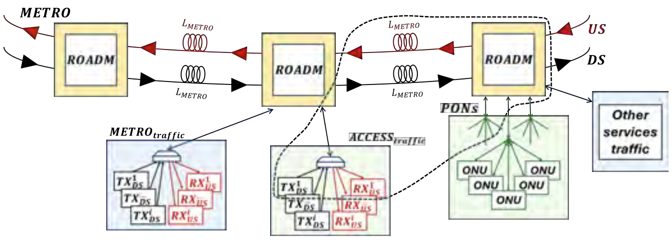

Fig. 1. The general Metro+Access convergence scenario considered in this paper, with ROADMs at the boundary between the two network segments. The dashed line highlights the network subsection that is experimentally demonstrated in the paper.

BiDi solution, just by reading the graph at lower ODN loss.

3. GENERAL CONTEXT AND EXPERIMENTAL SETUP

In this Section, we start with an overview of the general context and then we detail the implemented experimental setup. We consider the general scenario depicted in Fig. 1, where we assume that the metro and access network segments are merged by introducing a common dense wavelength division multiplexing (DWDM) coherent transmission technology in both segments (later in the paper we will also discuss the backward compatibility with current ITU-T PON standards). To achieve convergence, we consider the presence of ROADMs at the boundary between the two segments, following the architectures described and numerically investigated in our previous work [2]. In the experiments, we analyze the section included in the dashed line in Fig. 1, which consists of a single metro span, a ROADM and an ODN tree.

We consider a bidirectional transmission with a wavelength allocation in C-band since, besides being by far the most commonly used one for metro, it is also the only spectrum part that in the ITU-T PON wavelength allocation plan that is still mostly available (apart from CATV in some parts of the world, and for NG-PON2, which anyway for the moment is not largely used). As shown in Fig. 2, we focus on the G.694.1 ITU-T 100 GHz WDM grid, selecting channel 24 (λ_1^{DS} = 1558.17 nm) for the PON downstream (DS) direction and channel 25 (λ_2^{US} = 1557.36 nm) for the upstream (US) direction. In addition to these two modulated data channels, we fully populated the C-band spectrum inserting in the metro segments other 38 dummy channels spaced by 100 GHz (for a total of 40 WDM channels), generated by properly shaping ASE noise. We further assume that metro traffic uses 30 channels (from slots 26 to 55 of the ITU-T grid, blue in Fig. 3), while 10 channels (slots 16 λ_{16}^{ITU-T} = 1564.67 nm to 25 λ_{25}^{ITU-T} = 1556.55 nm, green in Fig. 3) are allocated to be terminated/generated in the access segment (including the two modulated US and DS signals).

The details of our experimental setup are shown in Fig. 3. The US L_{metro}, DS L_{metro} and L_{PON} fiber paths consist of three dark fiber links (16.5 km each) deployed in the city of Turin, Italy in a metropolitan telecom installation. The fibers connect two different locations: the POLITO PhotoNext Lab and the FiberCop lab. Each fiber passes through various cabinets in the city and many connectors, generating spurious extra-attenuation and back-reflections (typical in access installations) for a total fiber loss around 15 dB.

Two commercial coherent transceivers (Coherent TRX) in the PhotoNext Lab generate the 63 GBaud DS and US data streams for the bidirectional transmission configuration, at the aforementioned λ_1^{DS} and λ_2^{US} respectively. We programmed the Coherent TRX for 400G PM-16QAM or 200G PM-QPSK modulation (all data rate are here specified as net rates, so for instance the 400G means 400 Gbit/s net bit rate, while the line raw bit rate is around 504 Gbit/s). For the DS transmission (black solid lines in Fig. 3), a DWDM comb source consisting of ASE noise properly shaped by a Finisar 1000S waveshaper, generates 38 dummy channels (from ch. 16 to ch. 23 emulating other PON channels, and from ch. 26 to ch. 55 of the ITU-T 100 GHz grid emulating metro carriers) which are then coupled with the DS signal at λ_1^{DS}. Next, an EDFA amplifies these 39 WDM signals to achieve a total transmitted power on the metro segment equal to $P_{metro}^{DS} = 12$ dBm (about -4 dBm per channel). Since experimentally we could emulate propagation over only a single metro span (due to the lack of other ROADMs in our labs), in order to take into account the effect of the ASE noise accumulated on the several metro sections of a realistic network, we use the noise loading technique to impose an adjustable $OSNR_{metro}^{DS}$ and $OSNR_{RX}^{US}$, respectively at the beginning of the metro DS fiber path and at the input of the receiver in the US direction. ASE noise is generated in a 200 GHz bandwidth around channels 24 (DS) and 25 (US), filtered for improved flatness, amplified, and finally varied through a variable optical attenuator to change the resulting OSNR, defined on a bandwidth equal to the symbol rate.

After traveling along the 16.5 km L_{metro} DS fiber length, a 4-degree (4D) ROADM is used at FiberCop laboratory to properly route the 39 WDM channels. Each degree of the ROADM is made of the combination of an EDFA and a Wavelength Selective Switch (WSS) in the two directions, as depicted in Fig. 3. Each WSS introduces an attenuation $\alpha_{WSS} = 5$ dB. In the first degree (D1) the pre-amplifier (Pre) amplifies the 39 WDM channels to 22 dBm constant output power (about 6 dBm per channes) then the WSS is programmed to all-optically route channels 16 to 25 λ_{PON}^{DS} towards the access segment. In a real-traffic network, the remaining 30 channels (26 to 55) would be directed towards the

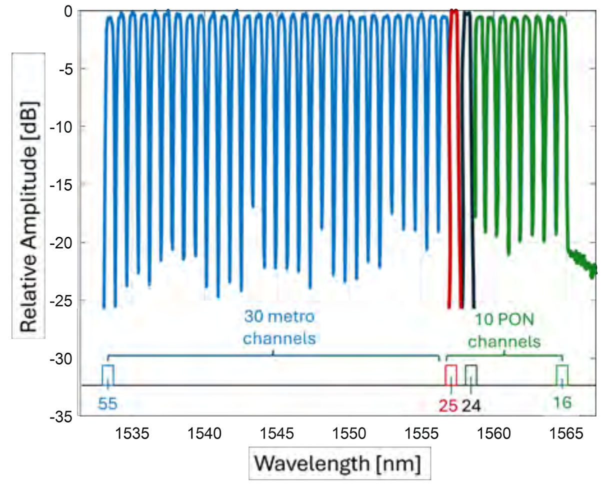

Fig. 2. Optical spectrum measured in the experiments with Optical Spectrum Analyzer (OSA) for the 40-channel WDM comb used in the metro segment (above) and allocation on the ITU-T grid (below). The PON DS and US signals are highlighted respectively in black and red.

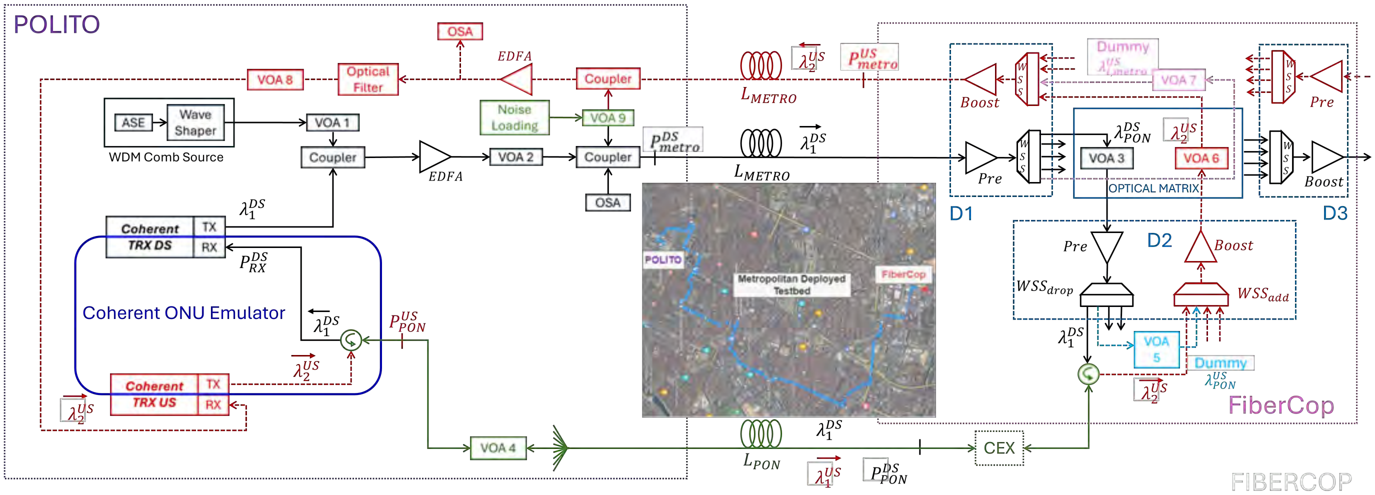

Fig. 3. Schematics of the full experimental setup, emulating the network subsection highlighted with a dashed line in Fig. 1. Black solid lines refer to the DS direction, while red dashed lines refer to the US direction. The green color refer to common elements in both directions. In the inset, the fiber path deployed in the city of Turin.

following metro section or dropped locally. Here, only for the sake of the experiments, we re-use and re-route them as dummy metro channels for the US direction, by coupling them with the US access data channels through the other WSS in D1, in the opposite direction.

The 10 λ_{PON}^{DS} allocated for the access segment are attenuated using Variable Optical Attenuator 'VOA 3', which is used to introduce a variable attenuation that experimentally emulates the optical connections inside the ROADM. We call this parameter optical matrix loss and indicate it as α_{OM} and we vary it in our experiments over a wide range. This choice is due to the many technological solutions that are today implemented inside ROADMs to optically interconnect the WSSs (passive splitter, optical switches or other filtering functions), each having a very different insertion loss. In the following Section, we present results also vs. α_{OM} so that we can show how different internal optical interconnection matrices technology would impact the overall physical layer performance. The 10 λ_{PON}^{DS} wavelengths are subsequently amplified at node D2 to ensure that the per channel power level at the output of the ROADM, after the output WSS_{drop}, is equal to $P_{PON}^{DS} = 11$ dBm, a typical value for the average transmitted power in current PON standards (such as XG-PON). In a real-traffic implementaiton, each λ_{PON}^{DS} would then be sent to a different PON. Here, due the hardware and fiber availability in our labs, we program thiss WSS_{drop} to separate the channel under test at λ_1^{DS} (that is sent to the rest of the access transmission chain) and the other 9 access wavelengths, that are coupled to λ_2^{US} in the other WSS_{add} in D2 and re-used as dummy channels in the US direction.

The DS modulated signal λ_1^{DS} under test propagates through another 16.5 km fiber span (the L_{PON} fiber) and a VOA (emulating the high loss introduced by a PON optical splitter), then reaches the detection side of the transmitting (Coherent TRX DS) coherent transceiver at the POLITO PhotoNext laboratory. In a realistic system, this receiver would be located inside a specific carrier-class ultra high-speed optical network unit ('premium' coherent ONU, highlighed in a blu box in Fig. 3). At both ends of the L_{PON} fiber two circulators are used to ensure bidirectional transmission of different λs in US and DS directions on the same simplex fiber. Lastly, 'VOA 4' is used at the receiver input to change the received optical power and thus emulate a variable loss optical distribution network (ODN). Specifically, we define here as ODN loss the difference in dB between the transmitted power P_{PON}^{DS} at the WSS_{drop} output and the received power P_{RX}^{DS} at the coherent receiver input, thus also including the insertion loss of the two circulators at both ends of the L_{PON} fiber.

In the US direction (red dashed lines in Fig. 3), a coherent transceiver (again highlighted in the coherent ONU blue box) generates the $\lambda_2^{US} = 1557.36$ nm signal, which in our experiment was either 400G PM-16QAM or 200G PM-QPSK for the upstream access data, emulating a completely simmetric DS/US rate in our experiments. The US signal then follows the same ODN path as the DS but in the opposite direction, entering the L_{PON} fiber with a power of $P^{US}PON = 3.7$ dBm. Also for the US case, the ODN loss is defined as the difference between the transmitted power P_{PON}^{US} and the power at the WSS_{add} input, thus it also includes the insertion loss of the circulator at the ROADM side. After the access segment ODN, λ_2^{US} reaches the ROADM D2 WSS, where it is merged by the WSS with the other 9 dummy PON channels, properly attenuated through 'VOA 5' for equalization purposes. In a realistic implementation of the metro-access scenario, as already mentioned for the DS, these PON channels would be related to other ODN trees provisioned in the same central office, which we only emulated in our experiment. The D2 booster (Boost) amplifies channels 16 to 25 of ITU-T grid (excluding channel N.24 used for DS) to a total global output power of 16 dBm. Similar to the DS, 'VOA 6' introduces different attenuation to obtain various α_{OM} values in the upstream case. The WSS in D1 would then combine these PON λs with the other signals traveling in the metro network, proceeding as pass-through carriers from D3 to D1 or originated in this FiberCop node. Since other metro spans are not implemented in our experiment, we re-use the DS metro dummy channels, properly attenuated through 'VOA 7', to emulate the 30 US metro channels to be transmitted toward POLITO node. 'VOA 7' and the WSS internal VOA are set to achieve a power equalization between channels and a transmitted power of $P_{metro}^{US} = 0$ dBm per wavelength after D1 booster amplification (about 16 dBm total transmitted power in the metro segment). Since metro networks use two separate fibers for data traffic in the two directions, the 39-channel US WDM comb at the D1 booster output travels along a different fiber with respect to the DS comb. On the receiver side in the PhotoNext lab, the same noise loading hardware used for the transmitter is employed to vary the received $OSNR_{RX}^{US}$ and emulate the effect of several metro spans on signal quality. Before detection, the US signal is amplified, filtered to isolate the channel under test (as done for any dropped carrier in a ROADM node), and attenuated to fix the received power to $P_{RX}^{US} = -7$ dBm.

The described US and DS transmissions are simultaneously tested to experimentally investigate the ultimate physical layer capabilities for a 63 GBaud bidirectional communication on the metro+PON fiber deployed testbed. We consider two different modulation formats: PM-16QAM at 400G net data rate and PM-QPSK at 200G.

4. EXPERIMENTAL RESULTS

In the following Subsections, we will present the main results of our large set of experiments, showing them in terms of maximum achievable ODN loss at a given BER target as a function of the OSNR in the metro segment, assuming different cases and different impairments. In particular, we will focus on:

- the effect of the optical matrix loss inside the ROADMs. We consider several values of its attenuation α_{OM}. In this way, we abstract our results both from specific component implementations of the ROADM optical connections between its WSS, and from the power equalization strategies used in DWDM metro architectures. In fact, depending on the specific internal interconnection logic, on the architecture and on the port-count, ROADMs complexity as well as their overall loss can vary considerably. For instance, a 1x20 route-and-select (R&S) ROADM has a lower insertion loss than a 1x9 broadcast-and-select (B&S) one. With the aim of making our analysis of the metro-access scenario as independent of the specific ROADM technology as possible, we vary α_{OM} inside a large dB range;
- the effect of unbalanced PON channels. We emulate different ONU distance ranges and different target losses for different ODN trees, setting a power-unbalance on the US PON channels;
- the effect of optical filtering in ROADMs. We program the WSS transfer function by setting the starting and ending frequencies of the selected DWDM optical spectrum via software, conventionally referring to this difference as the WSS bandwidth (BW) in this paper. In the main first round of experiments, WSS and received optical filter are set to 100 GHz bandwidth to minimize the effect of optical bandwidth limitations. However, in the next Sections we will also show the penalty due to non-ideal filtering;
- coexistence with legacy PONs. We analyze the impact of having legacy PON current technologies propagating simultaneously with the proposed coherent-PON approach.

A. Baseline performance in terms of ODN loss, OSNR and connection matrix optical loss

In this Subsection, we study the system performance in terms of achievable optical power budget of the access segment (α_{ODN}) as a function of the $OSNR_{metro}^{DS}$ for different values of the attenuation α_{OM} introduced by the ROADM. We do so by properly spanning the loss of the VOAs shown in Fig. 3 (in particular 'VOA 3' for α_{OM} and 'VOA 4' for α_{ODN}).

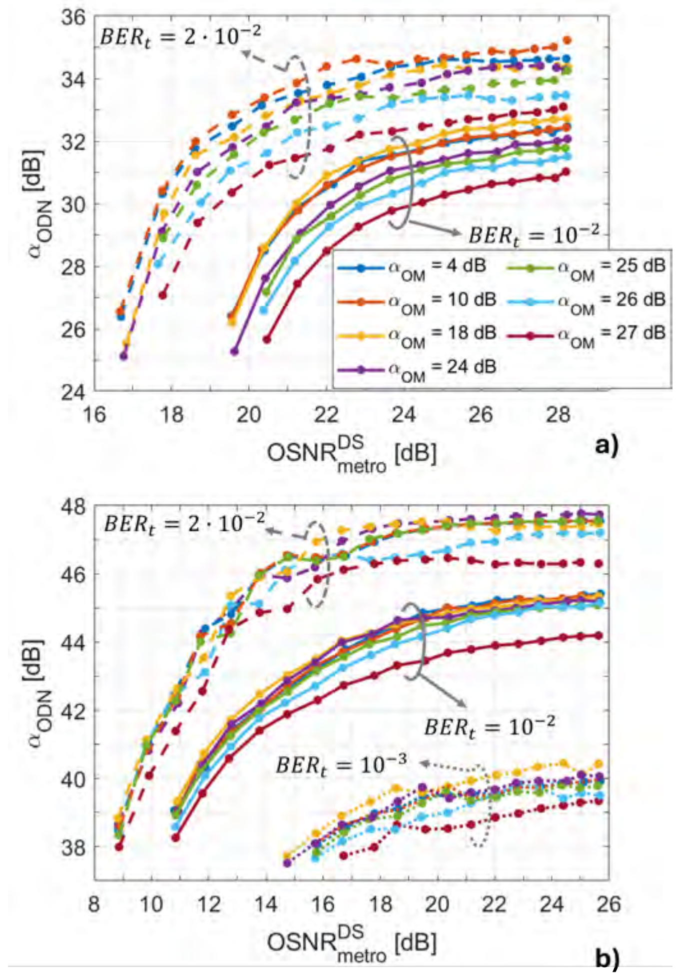

Fig. 4. ODN loss as a function of the metro $OSNR$ for $BER_t = 2 \cdot 10^{-2}$ (dashed), $BER_t = 10^{-2}$ (solid) and $BER_t = 10^{-3}$ (dotted) and several values of α_{OM} for a) 400G PM-16QAM, b) 200G PM-QPSK downstream transmission.

Fig. 4a and Fig. 4b show DS results for 400G PM-16QAM modulation and 200G PM-QPSK modulation, respectively, for three different BER target (BER_t) levels associated to three different possible implementations of the forward error correction (FEC) algorithm: 10^{-3} for a hard-decision (HD) FEC, 10^{-2} for a soft-decision (SD) FEC, and $2 \cdot 10^{-2}$ for an even more advanced SD-FEC (ASD-FEC). The figure illustrates the impact of α_{OM} on the ODN loss α_{ODN} defined as the difference between the D2 WSS_{drop} output power and the power at the DS receiver (including thus the insertion loss of the two circulators at either end of the optical fiber path of the PON).

In order to understand how to interpret the graphs in Fig. 4, let's start by assuming a minimum acceptable ODN loss $\alpha_{ODN} =$ 29 dB, as defined in current standards for the lower N1 class PON. Fig. 4a highlights that 400G transmission based on PM-16QAM modulation can reach $\alpha_{ODN} = 29$ dB with OSNR in excess of 22.5 dB and 18.5 dB, respectively for the considered SD-

FEC and ASD-FEC, in the worst case when $\alpha_{OM} = 27$ dB. This requirement on the OSNR relaxes to 20.5 dB and 17.5 dB, respectively, for the best considered case with $\alpha_{OM} = 4$ dB. Moreover, the system proves to be very robust, at high OSNR levels, even for extremely high α_{OM} values, with achievable ODN loss above 30 dB and 33 dB at the two FEC thresholds. Thus, the results referred to 400G PM-16QAM show that metro-access convergence is possible (α_{ODN}>29 dB for acceptable $OSNR_{metro}^{DS}$) for both FEC thresholds $BER_t = 10^{-2}$ and $BER_t = 2 \cdot 10^{-2}$ and for all tested α_{OM}. The actual $OSNR_{metro}$ values for both DS and US depends on each specific metro implementation and standard. Just to mention an example, the OpenROADM MSA in [19] specifies a large list of option: the one that is very close to our experimental setup is indicated in [19] as "W 200-400G 63.1 Gbaud Opt Spec", and would be largely compatible with the results of our experiments in terms of $OSNR_{metro}$.

Fig. 4b shows instead the results for 200G PM-QPSK DS transmission. The performance is remarkably improved, as expected, with respect to the 400G case, so that very high ODN loss in excess of 38 dB can be achieved even at the lowest considered BER target $BER_t = 10^{-3}$ for the HD-FEC. If we consider the higher $BER_t = 10^{-2}$ and $BER_t = 2 \cdot 10^{-2}$ thresholds, ODN loss can be as high as 44 dB and 46 dB, respectively for the SD-FEC and ASD-FEC algorithm, for $OSNR_{metro}^{DS}$ values above 23 dB and 16 dB at the highest 27 dB α_{OM}. However, even very low OSNR levels can ensure excellent α_{ODN} at the two highest BER thresholds. For instance, more than 38 dB α_{ODN} is possible for $OSNR_{metro}^{DS}$ equal to 11 dB and 9 dB, respectively for SD- and ASD-FEC. Furthermore, the impact of the optical matrix loss is moderate (less than 1 dB penalty on the ODN loss) at low OSNR and increases slightly at high OSNR values, resulting in a maximum 1.5 dB α_{ODN} penalty in the worst case with $\alpha_{ODN} = 27$ dB with respect to the lowest α_{ODN} =4 dB case at the highest considered OSNR.

As a general comment on the results shown in Fig. 4 for the DS direction, when the optical matrix loss is limited to practical highest values (e.g. a total 25 dB - including 15 dB related to the 1x32 splitting stage in a B&S ROADM plus 5 dB - or 10 dB - for extra loss associated to connections and filtering), the price to be paid in terms of maximum achievable ODN loss is always less than 2 dB in the 400G tranmission case, and is even lower than 1 dB for 200G transmission, regardless of the considered FEC technology.

In upstream, the coherent ONU would likely not be based on EDFA amplification, thus in our experiments its average output optical power was limited to a few dBm (3.8 dBm). Thus, we expect a reduction of the achivable ODN loss, also considering that the US signal is further attenuated along its path by the D2 WSS_{add} and, as a consequence, the optical power at the D2 booster amplifier input can be extremely low. Moreover, when α_{ODN} is high, our ROADM D2 booster is not able to comply with the 16 dBm total constant output power setting and the D1 booster also receives a lower power signal. The combined effects of optical amplification of low-power signals in D1 and D2 can strongly limit the OSNR available at the receiver. In fact, we show in Fig. 5a the measured maximum OSNR as a function of the ODN loss α_{ODN}. In the following Fig. 5b, we show the metro-access US transmission results in terms of $\Delta OSNR_{RX}^{US}$, defined as an OSNR margin, namely the difference between the OSNR required at a given BER_t in back-to-back (BtB) transmission and the maximum OSNR that can be obtained for any given α_{ODN} value in our US setup. In terms of impact of the optical matrix loss, we expect a similar behavior as in the DS direction. To confirm this we have analyzed the system performance in the 400G transmission case imposing three different α_{OM} values, 15.4 dB, 17.4 dB and 20 dB. However, due to the limited availability of the experimental equipment we could test 200G transmission with only one value of the matrix loss $\alpha_{OM} = 9$ dB (without however representing a real constraint, since the main limiting factor in upstream is ODN loss). It is worth noting here that varying α_{OM} in the US case is not trivial, as the system requires the DWDM signals to be power equalized at the D1 output (input of the metro segment), which involves an accurate setting of the attenuation introduced by 'VOA4', 'VOA5', 'VOA6' and 'VOA7' for each pair of the α_{ODN} and α_{OM} parameters. While in our experiments we obtain this DWDM power equalization manually, it is clear that it would require a dedicated control system in an actual network implementation.

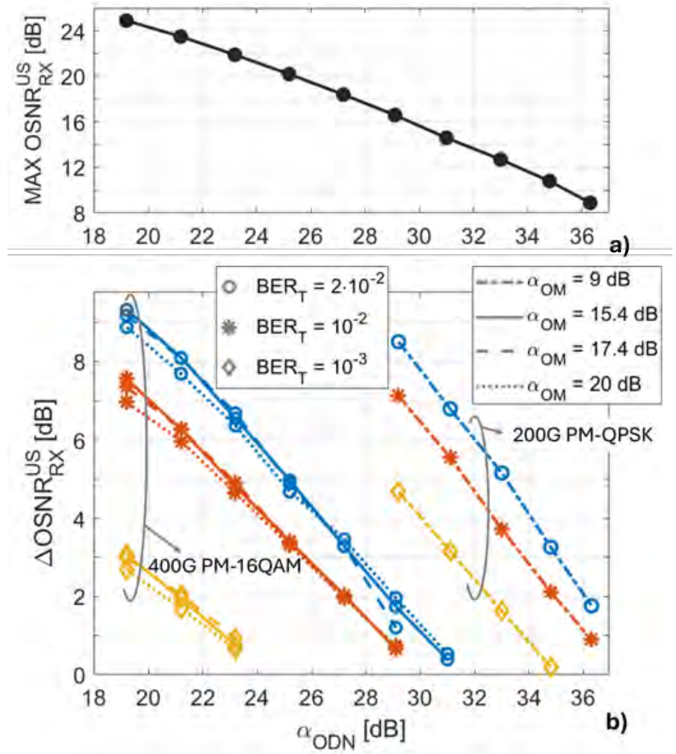

Fig. 5. a) Maximum $OSNR_{RX}^{US}$ achievable in BtB at each considered ODN loss. b) $\Delta OSNR_{RX}^{US}$ as a function of the ODN loss for $BER_t = 2 \cdot 10^{-2}$ (circle), $BER_t = 10^{-2}$ (asterisk) and $BER_t = 10^{-3}$ (diamond) and different values of α_{OM} for 400G PM-16QAM and 200G PM-QPSK uptream transmission.

The graph in Fig. 5b shows that $\Delta OSNR_{RX}^{US}$ reduces for increasing α_{ODN} as expected, since a progressively lower power signal requires a correspondingly higher gain and, therefore, a higher amount of ASE noise is introduced, mainly by the booster in D2, but also in D1. When using 400G PM-16QAM modulation, US communications can work at all three target BERs, but only the more advanced SD-FEC with $BER_t = 2 \cdot 10^{-2}$ can ensure that the minimum 29 dB α_{ODN} requirement is fulfilled. However, even in this best case, the OSNR margin is less than 2 dB. For 400G transmission, the results also show a negligible impact of the optical matrix loss, confirming that in US a ROADM attenuation up to 20 dB can be tolerated without significant penalty, as in the DS case. When using 200G PM-QPSK modulation, thanks again to the well-known robustness of QPSK modulation compared to 16-QAM, the system is able to provide ODN loss greater than 29 dB with acceptable margin at all three BER thresholds. Aa a "top level result", α_{ODN} is higher than 36 dB for the best ASD-FEC and allows for about 2 dB OSNR margin with respect to the about 9 dB maximum OSNR shown in Fig. 5a. At the lowest considered $\alpha_{ODN} = 29.2$ dB, the available OSNR margin ranges from 4.8 dB to 8.5 dB, respectively for HD-FEC and ASD-FEC. Please note that in the 200G transmission case the considered optical matrix loss is 9 dB. However, we have shown in the DS direction and in the US 400G case that the impact of this parameter on our metro-access system is negligible even for considerable α_{OM} values.

As a final and qualitative comment of this Section, we can summarize that in terms of ODN loss α_{ODN}, DS direction can largely satisfy the 29 dB ITU-T requirement in all considered situation even for 400-G transmission. On the contrary, US direction is really close to the α_{ODN}=29 dB target for 400G PM-16QAM transmission, while there are ample margins for 200G PM-QPSK.

B. The impact of power unbalance in US Direction

PON point-to-multipoint architecture is designed to be flexible enough to allow connection between the optical line terminal (OLT) and several final users that can be at different distances/attenuation from the OLT. Moreover, in the proposed metro-access converged scenario, each of the 10 PON λs is allocated for a different PON tree, that can have a different characteristics (e.g. splitting ratio, propagation distance, etc.) than the others. Therefore, in the US direction, this would give rise to a power unbalance among the PON channels that are received with uneven average power levels and, in our schematics, would be aggregated by the D2 WSS. In this Section, we study the effect of different upstream optical powers measured at the D2 WSS_{add} input, imposing a variable ΔP_{PON}, defined as the difference between the power of each dummy PON US signal and the US signal under test, introduced by increasing the attenuation on $\lambda_2^{US} = 1557.36$ nm through 'VOA 4' in Fig. 3 to decrease the US PON channel power. Each WSS_{add} port would come from a different PON ODN, and it is reasonable to assume different ODN losses between the PON tree under test and the neighbors (see inset Fig. 6b for specral-based explanation of the situation). To maintain the unbalanced equalization also at the input of the D1 WSS_{add}, we acted simultaneously on 'VOA 4', 'VOA 5' and 'VOA 6'.

Similarly to the previous Section for US performance, Fig. 6 shows the results in terms of $\Delta OSNR_{RX}^{US}$ as a function of the ODN loss α_{ODN} of the US signal for several ΔP_{PON} values and at the three different BER_t. As a reference, the blue curves for $\Delta P_{PON} = 0$ dB are the same results shown in Fig. 5 when channel equalization was ideal and no power unbalance was introduced.

For the 400G PM-16QAM modulation shown in Fig. 6a a slight impact of the power unbalance is observable. For a given α_{ODN} value, the available OSNR margin reduces for increasing ΔP_{PON}. For instance, when considering the ASD-FEC, at 29.2 dB ODN loss, the $\Delta OSNR_{RX}^{US}$ reduces from 1.9 dB to about 0.3 dB when the power of the PON channel under test is reduced to 8 dB below the power of the other dummy channels. The $\Delta P_{PON} = 8$ dB case is somewhat extreme and unrealistic, but shows that power unbalance can have an impact on 400G US transmission. For 200G PM-QPSK transmission, on the other hand, Fig. 6b shows no effect of the power difference between PON channels, confirming that 200G US communications can be robustly ensured at all the considered BER thresholds, with excellent ODN loss and OSNR margin, without requiring extremely high OSNR (see Fig. 5a).

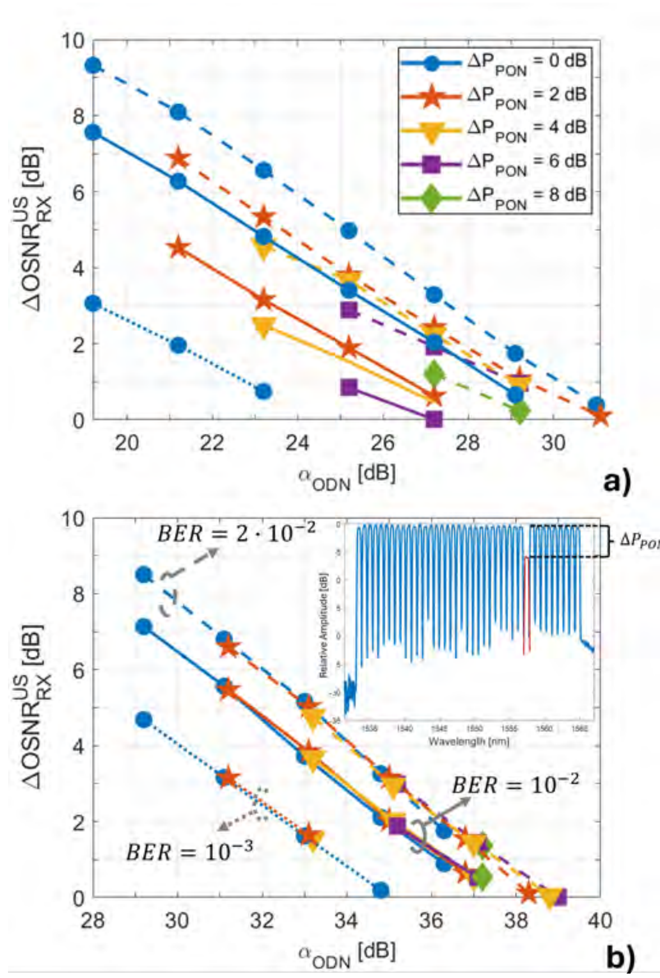

Fig. 6. $\Delta OSNR_{RX}^{US}$ as a function of the ODN loss for a) 400G PM-16QAM and b) 200G PM-QPSK at $BER_t = 2 \cdot 10^{-2}$ (dashed), $BER_t = 10^{-2}$ (solid) and $BER_t = 10^{-3}$ (dotted) and for different ΔP_{PON} values. Legend in a) applies to b) as well. BER indications in b) applies to a) as well. The inset in b) shows ΔP_{PON} definition inside the acquired spectrum (US signal in red).

In conclusion, this Subsection B shows some first-level considerations on the important topic of DWDM power equalization in the proposed metro-access converged architecture. For space and time limitation, we admit we only preliminarly introduced the topic

C. The impact of tight optical filtering

Another possible source of performance penalty in metro-access networks based on ROADMs may be related to the WSS optical filtering stages inside the device [10], for situation in which the end-to-end optical transfer function is band-limiting the actual transmitted signal spectrum. The rationals of this Subsection in a metro-access converged environment is related to two considerations:

1. for the upstream, the coherent-ONU transmitter laser may

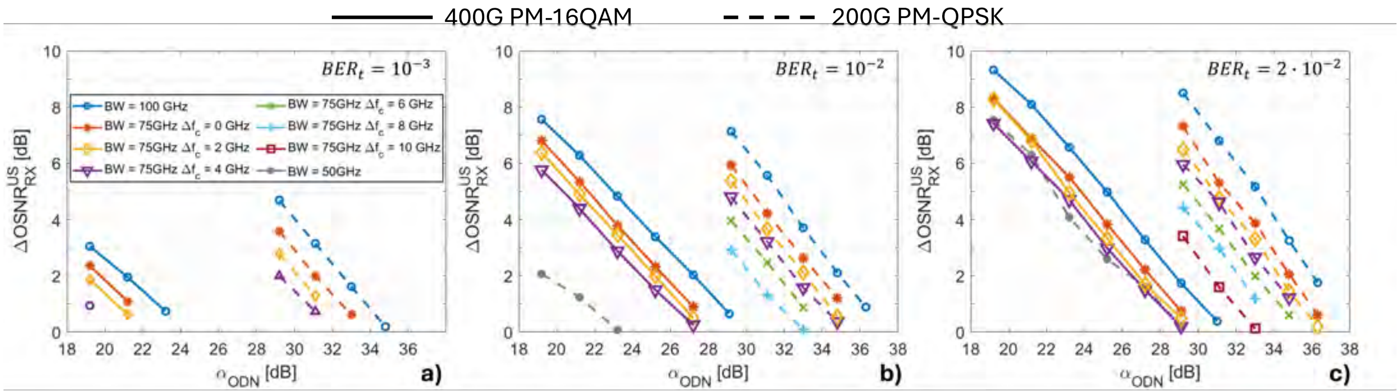

Fig. 7. $\Delta OSNR_{RX}^{US}$ as a function of the ODN loss for different WSS BW and Δf_c for 400G PM-16QAM (solid) and 200G PM-QPSK (dashed) at a) $BER_t = 10^{-3}$, b) $BER_t = 10^{-2}$ and c) $BER_t = 2 \cdot 10^{-2}$. Legend in a) applies to b) and c) as well.

be partially misaligned with respect to the WSS central wavelength, since future coherent-ONU, for cost reasons, may use lower grade optoelectronic components compared to long-haul coherent transceivers.

2. even though not studied in this paper for space limitations, future metro-access architectures may try to reduce as much as possible the optical spectrum dedicated to the access wavelengths, and thus use a narrower and more compact frequency spacing, again leading to potential filtering issues.

To this end, we already showed in previous works [10, 20] that a band-limited optical filtering can cause a penalty of several dB on the system performance, depending on the parameters describing the frequency response of the filter, such as bandwidth, steepness of the filter edges, offset with respect to the nominal central frequency, etc. In this Subsection, we study the effect of both optical filter bandwidth and central frequency offset (Δf_c between the central frequency of the transmission laser and the center of the WSS BW) of the WSS in the D2 degree in both DS and US directions. In previous Subsections, the WSS BW was set to a reference value equal to 100 GHz, a value broad enough to accommodate the whole 63 GBaud signal without any filtering penalty. Fig. 7 shows the $\Delta OSNR_{RX}^{US}$ as a function of α_{ODN} for different WSS bandwidths and for both considered modulation formats. Fig. 7a, Fig. 7b and Fig. 7c show the results for $BER_t = 10^{-3}$, $BER_t = 10^{-2}$ and $BER_t = 2 \cdot 10^{-2}$, respectively.

The blue curves in Fig. 7 represent the reference curves at 100 GHz already shown in Fig. 5 and Fig. 6. As the granularity of the used WSS allowed to vary the filter bandwidth only at 25 GHz steps, we reduced it to 75 GHz and 50 GHz. In the 75 GHz bandwidth case, we also analyzed the effect of a slight mismatch between the central frequency of the signal and that of the WSS, by introducing a frequency shift Δf_c up to 10 GHz.

For HD-FEC shown in Fig. 7a we could not perform measurements with a 50 GHz bandwidth WSS as the sensitivity curves do not cross $BER_t = 10^{-3}$ with either modulation scheme. With a 75 GHz WSS, on the other hand, we were able to observe a steady reduction of US communications performance. Nevertheless, at 200 Gbps, the system can still enable more than 29 dB ODN loss even with a 75 GHz WSS bandwidth and a 4 GHz central frequency offset. As we increase the FEC threshold the penalty due to optical filtering reduces slightly, allowing for frequency offset up to 8 GHz in the SD-FEC case of Fig. 7b, and even up to 10 GHz for the ASD-FEC in Fig. 7c, while still providing $\alpha_{ODN} > 29$ dB with reasonable OSNR margin in the 200G PM-QPSK transmission case. Surprisingly enough, also a 50 GHz bandwidth WSS enables successful 200G US communications with the two SD-FEC algorithms, although the achievable ODN loss can hardly reach the desired 29 dB. PM-16QAM modulation is again very critical, with admissible α_{ODN} further reducing below 29 dB due to narrow filtering, confirming that 400 Gbps in the US direction is not an option for current PON ODN loss needs, but it can be feasible in hypothetical next-generation super-high-speed PON on shorter distances or with a reduced splitting factor, when the requirement on the acceptable α_{ODN} can be relaxed to allow a lower total power budget. For instance, an acceptable $\alpha_{ODN} = 25$ dB would enable 400G US transmission with a reasonable OSNR margin greater than 2 dB, even for 75 GHZ WSS BW and Δf_c up to 2 GHz (SD-FEC) or 4 GHz (ASD-FEC).

Due to the limited availability of the experimental equipments, we were not able to investigate the effect of the Δf_c parameter in the DS direction, but we could only study the effect of a reduced 75 GHz WSS BW. Fig. 8 shows the achievable ODN loss as a function $OSNR_{metro}^{DS}$ for the two modulation formats, for the three considered BER_t and for two filter BW when $\alpha_{OM} = 25dB$. All the curves are perfectly superimposed showing a negligible impact of the optical filter contraction, thus confirming that DS metro-access communications is an exceptionally promising solution for next-generation all-coherent networks, even at very high 400 Gbps bit rates.

D. Preliminary investigation on the coexistence with ITU-T legacy PON standards

In previous Sections, we analyzed a transmission situation using only coherent technologies also in the access segment: this is the architecture we indicated as "disruptive" in our previous simulative paper [2], where we also discussed an "evolutionary architecture" based on a mix of legacy ONUs and coherent ONUs, which will very likely be the first one to be implemented if metro-access convergence take momentum in the near future. Consequently, in this Subection, we test the coexistence of a fully coherent PON communication scheme with legacy PON transmission. We admit that this topic would require a much larger amount of research work, and that the following is just a preliminary experimental investigation on this topics. Specifically, we incorporate a legacy XGS-PON transmission within the

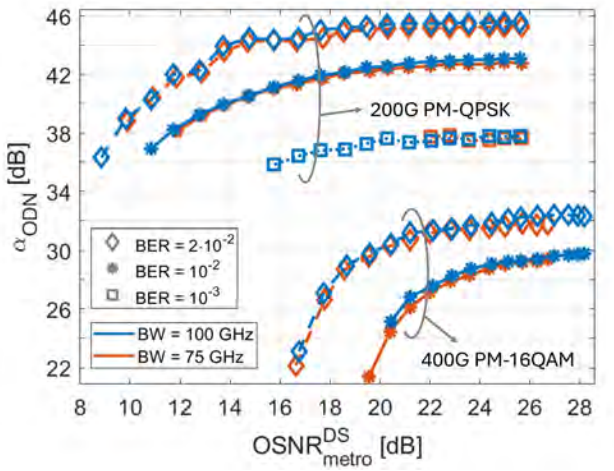

Fig. 8. Downstream filtering effects: α_{ODN} vs. $OSNR^{DS}_{metro}$ at three BER_t for two modulation formats and for 100 GHz (red) and 75 GHz (blue) WSS bandwidth.

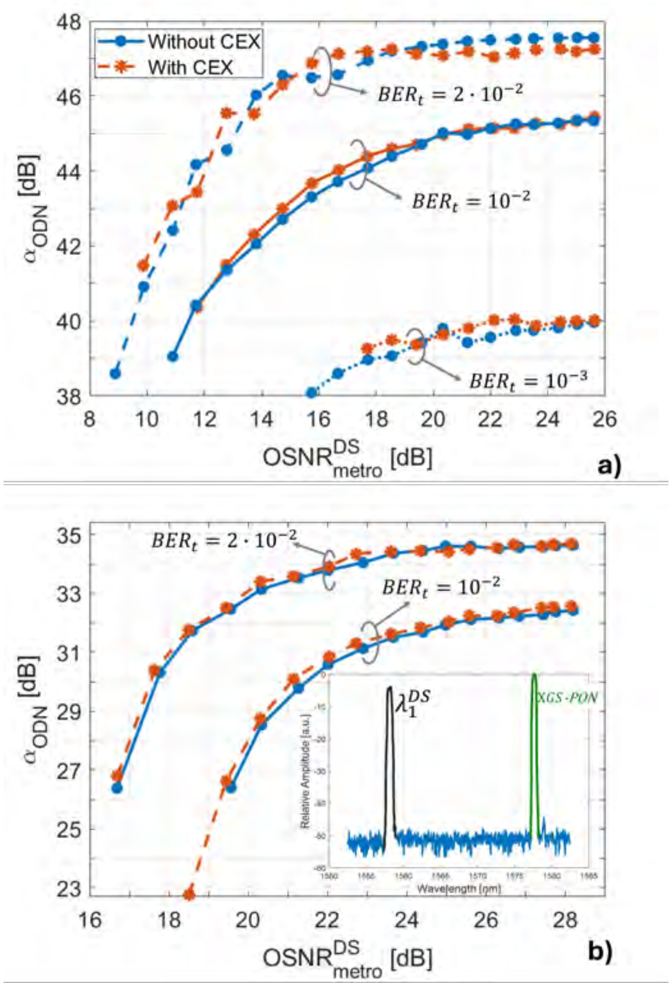

Fig. 9. Downstream CEX comparison: α_{ODN} vs. $OSNR^{DS}_{metro}$ at α_{OM}=10 dB with (dashed orange) and without (solid blue) the coexistent element. a) 400G PM-16QAM, b) 200G PM-QPSK for different BER target. Legend in a) applies to b) as well.

access segment, using a commercial coexisting element (CEX). For this experimental analysis, we include the CEX illustrated as a dashed box at the input/output of degree D2 in Fig. 3. Here, our goal is to characterize, in the presence of XGS-PON wavelengths, the coherent DS transmission in terms of α_{ODN} versus $OSNR^{DS}_{metro}$, for a single representative value of matrix loss $\alpha_{OM} = 10$ dB. In Fig. 9 we compare performance in the presence and absence of the XGS-PON. Results show that for all the analyzed modulation formats (400G PM-16QAM in Fig. 9a and 200G PM-QPSK in Fig. 9b) and BER targets, the curves for the DS full coherent transmission are superimposed. This indicates that coexistence between the full coherent and legacy PON is possible, as there is no crosstalk between the two propagating PON signals. These findings can be ascribed to the fact the two transmissions use separate λs that are displaced by almost 20 nm on the wavelength axis, $\lambda_1^{DS} = 1558.17$ nm for the coherent and $\lambda^{DS}_{XG-PON} = 1577$ nm for the XG-PON, as shown in the inset of Fig. 9b.

As final comment, it is worth underlining that the curves in Fig. 9 are perfectly superposed as α_{ODN} is computed as the difference between the power at the output of the WSS_{drop} and the power at the DS receiver input. Therefore, it also includes the insertion loss of the CEX (about 1 dB) that needs to be properly taken into account for a correct design of the network.

5. CONCLUSIONS

We present in this paper a vast set of experimental results on the new topic of metro-access convergence enabled by coherent transmission technologies also for the access part, and by wavelength-routing in ROADMs. The rationale of this paper is to show the ultimate physical layer limitation and constraints. We acknowledge that this is only an "introductory" work to start discussing this new topic. Clearly, besides the techno-economic considerations, such as those concerning if and when coherent transceivers reach a cost compliant with the access segment or if and when access terminations will require hundred of Gbps capacity, several technical issues are still open, such as:

- which type of multiplexing approach would be best for the upstream, i.e. single-carrier TDMA, digital subcarrier multiplexing (DSCM) or a mix TDMA+DSCM. If TDMA is used in the upstream, this opens an issue for EDFA gain transients;
- which wavelength allocation plan would be best for metro and access traffic;
- DWDM power balancing due to both the usual EDFA-induced gain tilt in the metro part, and the power imbalances in upstream due to the very heterogeneous ODN loss values in the access;
- last but not least, an all-optical converged metro-access scenario would require an important re-thinking of network level control and orchestration.

ACKNOWLEDGMENTS

This work was partially funded by the European Union Horizon Europe research and innovation programme, under the ALLEGRO Project (Contract No. 101092766). Experiments were performed using the PhotoNext Center facilities at Politecnico di Torino (www.photonext.polito.it).

REFERENCES

1. Y. Hu et al., "All-optical metro-access integration network bidirectional transmission enabled by coherent digital subcarrier multiplexing," in *IEEE/OPTICA Journal of Optical Communications and Networking*, vol. 17, no. 1, pp. 58-70, January 2025,
2. G. Rizzelli et al.,"Architecture and Scalability of Future Coherent Metro+PON Converged Networks", accepted for publications in *IEEE/OPTICA Journal of Optical Communications and Networking*
3. G. Rizzelli and R. Gaudino, "Planning tools for next-generation DSP-based passive optical networks above 50G [Invited Tutorial]," *IEEE/OPTICA Journal of Optical Communications and Networking*, vol. 16, no. 7, pp. C88-C96, 2024.
4. ITU-T G.suppl.VHSP "PON transmission technologies above 50 Gb/s per wavelength", https://www.itu.int/ITU-T/workprog/wp_item.aspx?isn=18554, accessed on December 2024.
5. Z. Jia, H. Zhang, K. Choutagunta and L. A. Campos, "Coherent passive optical network: applications, technologies, and specification development [Invited Tutorial]," in *IEEE/OPTICA Journal of Optical Communications and Networking*, vol. 17, no. 1, pp. A71-A86, January 2025,
6. G. Rizzelli *et al.*, "Scaling Laws for Unamplified Coherent Transmission in Next-Generation Short-Reach and Access Networks," *IEEE J. of Light. Techn.*, vol. 39, no. 18, pp.5805-5814, 2021.
7. I. B. Kovacs, M. S. Faruk, A. Wonfor and S. J. Savory, "200 Gb/s/ Bidirectional Coherent PON Solutions Demonstrated Over Field Installed Fiber," in IEEE Photonics Technology Letters, vol. 36, no. 17, pp. 1089-1092, 1 Sept.1, 2024.
8. M. Ruffini et al., "Access and metro network convergence for flexible end-to-end network design [invited]," in *IEEE/OPTICA Journal of Optical Communications and Networking*, vol. 9, no. 6, pp. 524-535, June 2017,
9. M. Casasco et al., "Experimental Demonstration of a 400 Gb/s Full Coherent Transmission in an in-field Metro-Access scenario," 2023 23rd International Conference on Transparent Optical Networks (ICTON), Bucharest, Romania, 2023, pp. 1-4.
10. G. Rizzelli, P. Torres-Ferrera, A. Napoli and R. Gaudino, "Filtering Effects Characterization in Metro-Access Networks and Future High-Speed Coherent Optical Communication Schemes," *Journal of Lightwave Technology*, submitted, June 2024.
11. G. Rizzelli, et al., "Experimental Demonstration of In-Field 400G Coherent Metro-Access Convergence," in *Proc. of Optical Fiber Communications Conference (OFC)*, San Diego CA, 2024.
12. G. Rizzelli, M. Casasco, A. Pagano, E. Riccardi, V. Ferrero and R. Gaudino, "Demonstration of Converged Metro+Access Bidirectional Transmission Using Coherent Transceivers and ROADMs" accepted for publications in *OFC2025*
13. H. Zhang, Z. Jia, L. A. Campos and C. Knittle, "Experimental Demonstration of Rate-Flexible Coherent PON Up to 300 Gb/s," in *IEEE/OPTICA Journal of Lightwave Technology*, vol. 42, no. 16, pp. 5440-5449, 15 Aug.15, 2024,
14. D. Welch, A. Napoli, J. Back, W. Sande, J. Pedro, F. Masoud, C. Fludger, T. Duthel, H. Sun, S. J. Hand et al., "Point-to-multipoint optical networks using coherent digital subcarriers," *Journal of Lightwave Technology*, vol. 39, no. 16, pp. 5232–5247, 2021.
15. G. de Valicourt et al., "Distributed fast optical packet power equalization for efficient WDM packet switched networks," 2012 38th European Conference and Exhibition on Optical Communications, Amsterdam, Netherlands, 2012
16. J. M. D. Mendinueta, S. Shinada, H. Furukawa and N. Wada, "Ultra-high-capacity optical packet switching networks with coherent polarization division multiplexing modulation formats and related technologies," 2017 19th International Conference on Transparent Optical Networks (ICTON), Girona, Spain, 2017.
17. M. M. Hosseini, J. Pedro, A. Napoli, N. Costa, J. E. Prilepsky and S. K. Turitsyn, "Optimized design of filterless horseshoe networks exploiting point-to-multipoint coherent transceivers," in Journal of Optical Communications and Networking, vol. 15, no. 9, pp. 569-578, 2023.
18. Z. Vujicic et al., "Toward Virtualized Optical-Wireless Heterogeneous Networks," *IEEE Access*, vol. 12, pp. 87776-87806, 2024.
19. OpenROADM MSA ver. 7.0 specification (last accessed January 2024) https://github.com/OpenROADM/OpenROADM_MSA_Public/wiki/files/20240307_open-roadm_msa_specification_ver7.0.xlsx
20. G. Rizzelli, P. Torres-Ferrera and R. Gaudino, "An Analytical Model for Coherent Transmission Performance Estimation After Generic Jones Matrices," *Journal of Lightwave Technology*, vol. 41, no. 14, pp. 4582-4589, 2023.